



## New redox anion receptors based on calix[4]pyrrole bearing ferrocene amide

Wenzhi Yang<sup>a</sup>, Zhenming Yin<sup>a,b</sup>, Chun-Hua Wang<sup>a</sup>, Chengyun Huang<sup>a</sup>, Jiaqi He<sup>a</sup>, Xiaoqing Zhu<sup>a</sup>, Jin-Pei Cheng<sup>a,\*</sup>

<sup>a</sup> Department of Chemistry, State Key Laboratory of Elemento-Organic Chemistry, Nankai University, Tianjin 300071, China

<sup>b</sup> College of Chemistry and Life Science, Tianjin Normal University, Tianjin 300387, China

### ARTICLE INFO

#### Article history:

Received 4 February 2008

Received in revised form 8 July 2008

Accepted 11 July 2008

Available online 16 July 2008

#### Keywords:

Anion recognition

Calix[4]pyrrole

Crystal structure

Redox receptor

Theoretical calculation

### ABSTRACT

Two redox anion receptors based on calix[4]pyrrole and ferrocene have been synthesized. The electrochemical investigation revealed that these compounds can be response to the anions with different shifts of Fc/Fc<sup>+</sup> couple. With the <sup>1</sup>H NMR titration study, the selectivity to F<sup>-</sup> and AcO<sup>-</sup> ions in CD<sub>3</sub>CN solution was confirmed. The conformations of the mono-aromatic *meso*-substituted calix[4]pyrroles, which were the synthetical intermediate of the ferrocene based receptors, and their anion complexes in the solid state have also been studied by single X-ray crystallography, and the rationality of the crystal conformations was proved by theoretical study.

© 2008 Elsevier Ltd. All rights reserved.

## 1. Introduction

The research on anion recognition has attracted rapidly growing attention recently due to the important roles of anions in many scientific areas such as chemistry, biology, therapeutics, ecology, pharmacology, and in industries.<sup>1,2</sup> As the significance of qualitative and quantitative information on anion recognition has become more and more visible, lots of interesting anion-hosting molecules were developed and their binding properties were more vigorously studied.<sup>1,2</sup> Among the anion receptors reported in the literature, calixpyrroles should be of particular interest since they showed good binding capability both in the solution and in the solid phase.<sup>3,4</sup>

However, unlike simple calixpyrroles, the synthesis of their derivatives often turned out to be not so straightforward. For example, the synthesis of the important *meso*-substituted series in the calixpyrrole family, which showed higher affinity to anions and had versatile reporter groups, was reported only in limited cases.<sup>5–16</sup> Furthermore, their binding behaviors were even less investigated. In these work, some *meso*-hook derivatives of calix[4]pyrrole have been synthesized and characterized<sup>13–16</sup> while the mono-*meso* aromatic-substituted calix[4]pyrrole attracted more attention because of the cooperation ability of the aromatic group to the anions binding progress. In the research of second generation calixpyrrole,<sup>5</sup> Sessler and co-workers employed

3-aminophenylcalix[4]pyrrole **3** as the substrate to construct three anion receptors. The unique character of these compounds was that they supported additional binding sites that could dramatically increase the binding capability to anions. These receptors could be treated as the analogs of lariat crown esters, whose recognition mechanism for ions was also the cooperation of the original ion receptor and the additional binding sites.

In the present work, a new type of redox anion receptors based on calix[4]pyrrole and ferrocene has been synthesized and characterized. The electrochemical investigation revealed that these compounds can respond to the anions with the different shifts of Fc/Fc<sup>+</sup> couple and the selectivity to F<sup>-</sup> and AcO<sup>-</sup> ions in CD<sub>3</sub>CN solution was confirmed with the <sup>1</sup>H NMR titration study. The conformations of the mono nitrobenzene-substituted calix[4]pyrroles and their anion complexes in the solid state have also been studied by X-ray single crystal diffraction, and the rationality of the crystal conformations was proved by theoretical study.

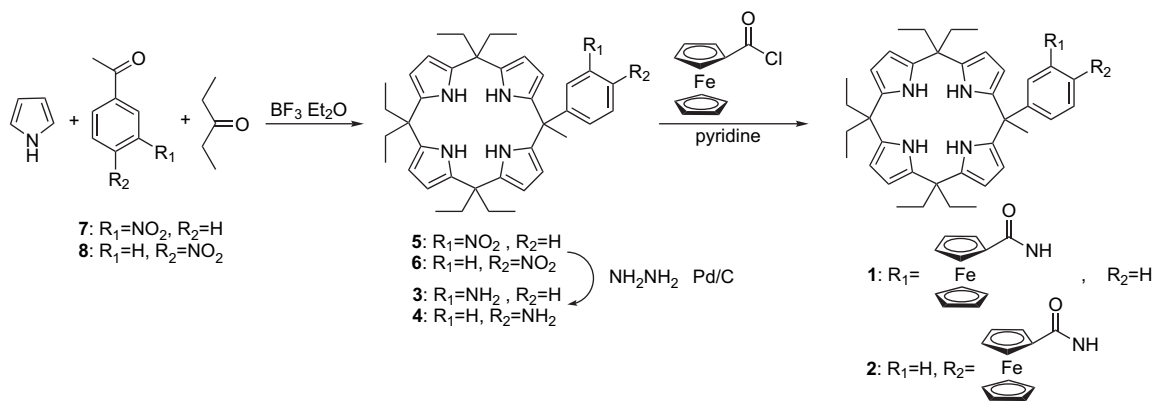
## 2. Result and discussion

### 2.1. Synthesis

The nitrobenzene-substituted calix[4]pyrroles **5** and **6** were prepared by the co-condensation of nitroacetophenone **7** (or **8**), pentan-3-one, and pyrrole in the presence of BF<sub>3</sub>·Et<sub>2</sub>O (Scheme 1). Then, **5** and **6** were reduced to the corresponding amine derivatives **3** and **4** by hydrazine hydrate under the catalysis of Pd/C. The ferrocenoyl chloride was obtained conveniently when triphosgene was

\* Corresponding author.

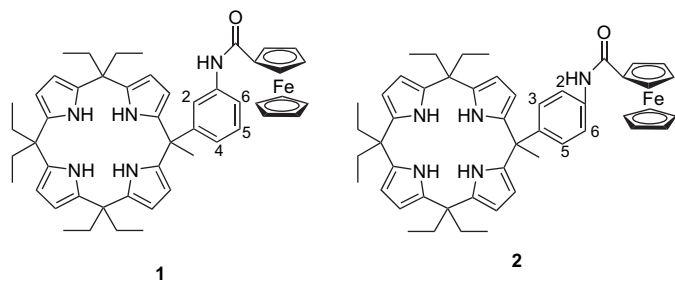
E-mail address: [chengjp@nankai.edu.cn](mailto:chengjp@nankai.edu.cn) (J.-P. Cheng).



Scheme 1. The synthetic route of receptor **1** and **2**.

reacted with ferrocene carboxylic acid in methylene dichloride at room temperature in the presence of triethylamine and DMAP.<sup>17</sup> The reaction between aminobenzene-substituted calix[4]pyrrole **3** (or **4**) and ferrocenoyl chloride in CH<sub>2</sub>Cl<sub>2</sub> in the presence of pyridine gave the receptor **1** (or **2**) successfully.

Compound **3** was an important intermediate compound and has been used in the synthesis of functional calixpyrrole. It was prepared in two steps from Cbz-protected 3-aminoacetophenone, pentan-3-one, and pyrrole in the presence of BF<sub>3</sub>·Et<sub>2</sub>O and followed by deprotonation of the initial product by catalytic hydrogenation<sup>5</sup> or 40% aqueous KOH in MeOH.<sup>18</sup> Herein, the synthetic route was shortened from three steps (including the preparation of Cbz-protected 3-aminoacetophenone) to two relatively simple steps with quite high total yield.



## 2.2. Electrochemical study

The electrochemical properties of the anion receptors **1** and **2** were investigated by cyclic voltammetry (CV) and square-wave voltammetry (SWV) in CH<sub>3</sub>CN (Fig. 1). The receptor was firstly scanned between +300 and –100 mV (vs Fc/Fc<sup>+</sup>), and a reversible Fc/Fc<sup>+</sup> wave was observed. While the cyclovoltammogram was scanned between +800 and –100 mV, a further oxidation wave appeared, which could be attributed to the calixpyrrole redox-activated center. The Fc/Fc<sup>+</sup> redox potentials of the receptors are summarized in Table 1. The fluoride induced the greatest cathodic shift of the Fc/Fc<sup>+</sup> couple around the halide, which was accompanied by chloride and bromide in turn. Among the complex anions, similar with the former literature,<sup>10</sup> the dihydrogenphosphate caused the largest cathodic shift, which was larger than the acetate and even larger than the halide. Additionally, the hydrogen sulfate caused a little anodic shift.

## 2.3. <sup>1</sup>H NMR titration study

The <sup>1</sup>H NMR titrations were also employed to study the binding properties of the receptors **1** and **2** in CD<sub>3</sub>CN (Fig. 2).

For **1**, with the addition of the fluoride, the signals of the pyrrole NHs disappeared until the new signals appeared at 12.3 ppm, which represented the formation of the stable complexes. Meanwhile, the upfield shifts of the signal of C<sub>2</sub> and C<sub>4</sub> protons of receptor **1** were observed dramatically. The addition of dihydrogenphosphate caused the same changes in the spectra, except for the disappearance of the amide NH and the attractive shifts of C<sub>6</sub> proton and ferrocene protons when the anion was

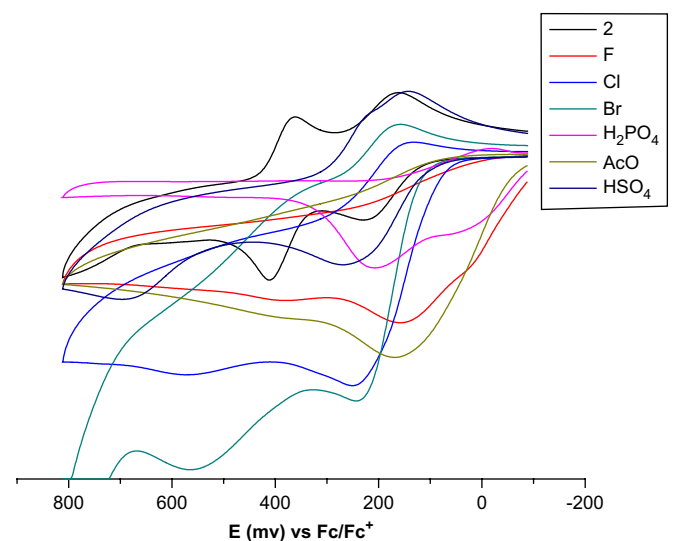
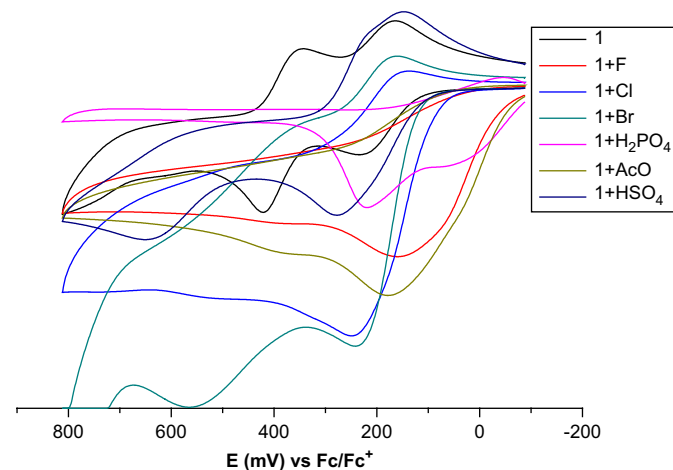


Figure 1. Cyclic voltammograms of **1** (top) and **2** (bottom) recorded in CH<sub>3</sub>CN (0.1 mol/l) *n*-Bu<sub>4</sub>NF<sub>6</sub> electrolyte.

**Table 1**  
Binding and electrochemical properties of compounds **1** and **2**

Anion <sup>a</sup>	Receptor <b>1</b>			Receptor <b>2</b>		
	$K_a^b$	$E_{1/2}$ (mV) <sup>c</sup>	$\Delta E$ (mV) <sup>c</sup>	$K_a^b$	$E_{1/2}$ (mV) <sup>c</sup>	$\Delta E$ (mV) <sup>c</sup>
No anion	N/A	196	N/A	N/A	192	N/A
F <sup>-</sup>	>100,000	80	116	>100,000	112	80
Cl <sup>-</sup>	3600	164	32	5300	160	32
Br <sup>-</sup>	80	200	-4	150	196	-4
H <sub>2</sub> PO <sub>4</sub> <sup>-</sup>	770	54	142	1900	60	132
CH <sub>3</sub> COO <sup>-</sup>	>100,000	120	76	>100,000	112	80
HSO <sub>4</sub> <sup>-</sup>	ND	208	-12	ND	200	-8

<sup>a</sup> Used in the form of their (*n*-Bu<sub>4</sub>N)<sup>+</sup> salts.

<sup>b</sup> Association constants for anion binding, recorded in CD<sub>3</sub>CN, errors <20%, determined from  $\Delta(\delta)$  [ppm] pyrrole  $\beta$ -CH since the signal of pyrrole N-H became obscure during the titration.

<sup>c</sup> Determined in CH<sub>3</sub>CN containing 0.1 mol/L *n*-Bu<sub>4</sub>NPF<sub>6</sub> as the supporting electrolyte. Solutions of **1/2** were  $1 \times 10^{-3}$  mol/L and potentials were determined with reference to Fc/Fc<sup>+</sup>.  $E_{1/2}$  values obtained from SWVs.

added. It revealed that the binding of receptors to the dihydrogenphosphate was profound and the multi-site binding, hydrogen bonds from calixpyrrole NH, amide NH, and ferrocene C–H, was dominated. The acetate also caused significant changes in the <sup>1</sup>H NMR of the receptor **1** and the whole process seemed like the binding process of the fluoride, which has been announced in the former publications.<sup>18,19</sup> Unlike the dihydrogenphosphate, the amide NH didn't disappear at all, which indicated that the calix[4]pyrrole was the main binding site. A clear doublet peak at 10.8 ppm suggested that the formation of the receptor–acetate complex was very stable, which maybe attributed to the relative small radius (oxygen vs chloride) and simple geometry (acetate vs dihydrogenphosphate).

With the addition of the chloride, similar phenomenon was observed as the fluoride titration except for the smaller shifts of all protons. These can be attributed to the larger radius of the anions that do not fit in the cavity of the calix[4]pyrrole and the relatively lower charge density that weaken the hydrogen bond. The bromide and the hydrogen sulfate caused only little changes in the spectra.

The non-linear fitting of the titration results with the WinEQNMR program<sup>20</sup> afforded associated constants of the

receptors, which are summarized in Table 1. It is clear that the binding constants of receptors **1** and **2** were higher than the octa-methylcalix[4]pyrrole even in acetonitrile. On the other hand, the polarized solvent may hamper the aggregations of the hosts for the formation of intermolecular hydrogen bond and let the receptor to bind the anions more efficiently. Compared with the mono-substituted analogs, **1** and **2** also showed larger binding affinities to the anions, which could be attributed to the relatively smaller *meso*-substituted group (ethyl vs cyclohexanyl, phenyl vs ferrocene) and much efficient cooperation of the phenyl group, which was more close to the calix[4]pyrrole moiety. The constants also showed that the receptors have a selective recognition toward F<sup>-</sup> and AcO<sup>-</sup>. It is inconsistent with the electrochemical investigation. Same phenomena were also observed by Gale.<sup>10,23</sup> It may due to that H<sub>2</sub>PO<sub>4</sub><sup>-</sup> can interact more with ferrocene group and phenyl group whereas less interaction for F<sup>-</sup> and AcO<sup>-</sup> (Fig. 2).

#### 2.4. Single crystal study

In order to explain the binding behavior more exactly, the single crystals of the receptors and their anions complexes were obtained (Table 3). In fact the crystals of **5** and **6** and the complexes were obtained to illustrate the binding mode of the complexes because of the difficulty to acquire the single crystals of the receptors **1** and **2** and their complexes with anions.

The <sup>1</sup>H NMR titration experiments of the substrates **5** and **6** were not realized due to their poor solubility in CD<sub>3</sub>CN at room temperature. Fortunately, the same experiments were succeeded in CDCl<sub>3</sub> and DMSO, and the same phenomena, which in accord to **1** and **2** during the titrations that the aromatic C–Hs shifted upfield on the addition of the anions, were observed.

The suitable single crystal of **5** was obtained from hot CH<sub>3</sub>CN solution of **5**, while the single crystals of **6** were also obtained by the similar process in hot CH<sub>3</sub>CN and hot acetone. All three single crystals adopted distorted 1,3-alternative conformations (Figs. 3–5), which were the common cases of the unsubstituted-calix[4]pyrroles<sup>21</sup> and even the mono-aromatic *meso*-substituted calix[4]pyrrole in Gale's work.<sup>10</sup> In all three crystals, the phenyl

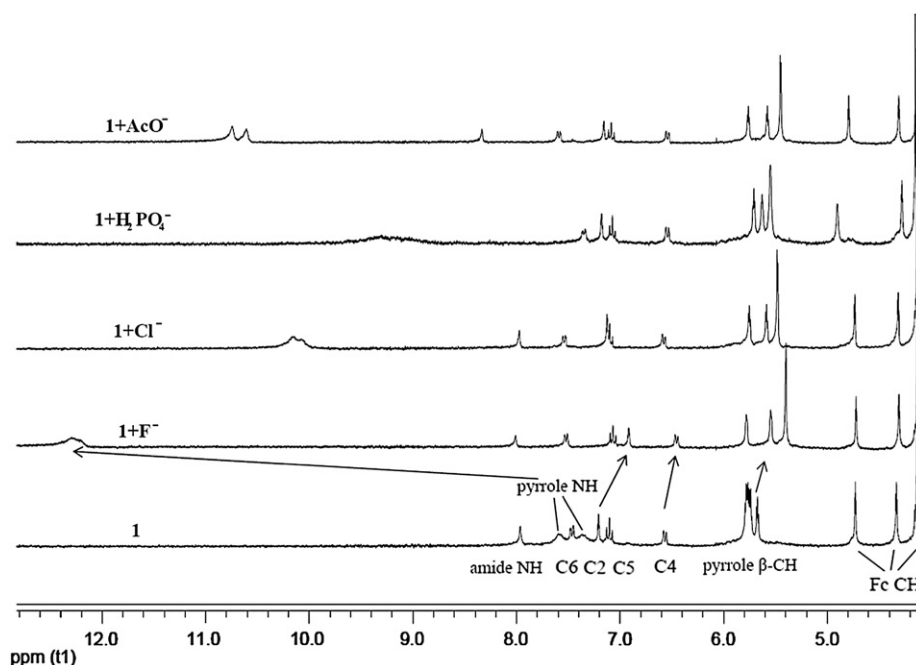


**Figure 2.** <sup>1</sup>H NMR spectra of compound **1** in CD<sub>3</sub>CN solution on addition of 1 equiv of tetrabutylammonium anions.

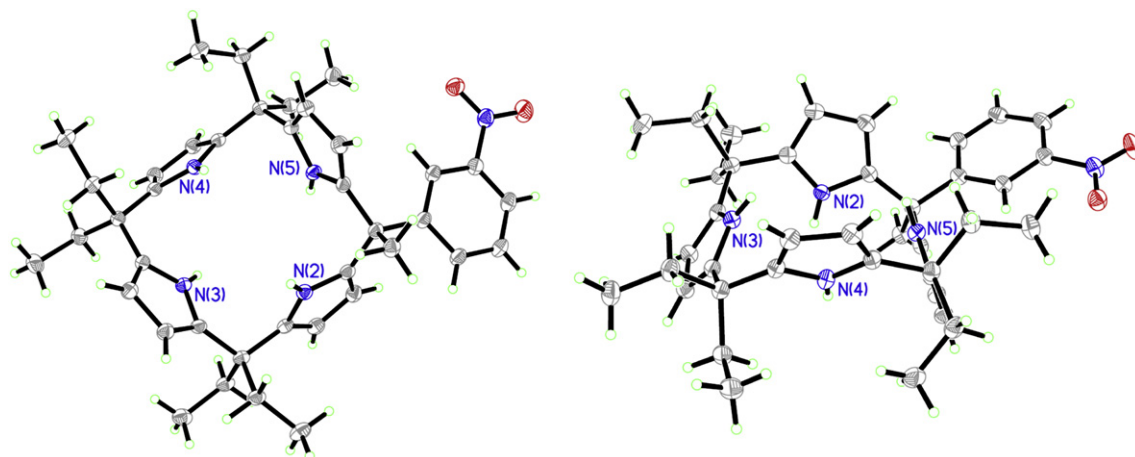


Figure 3. Top view (left) and side view (right) of the X-ray structure of **5**.

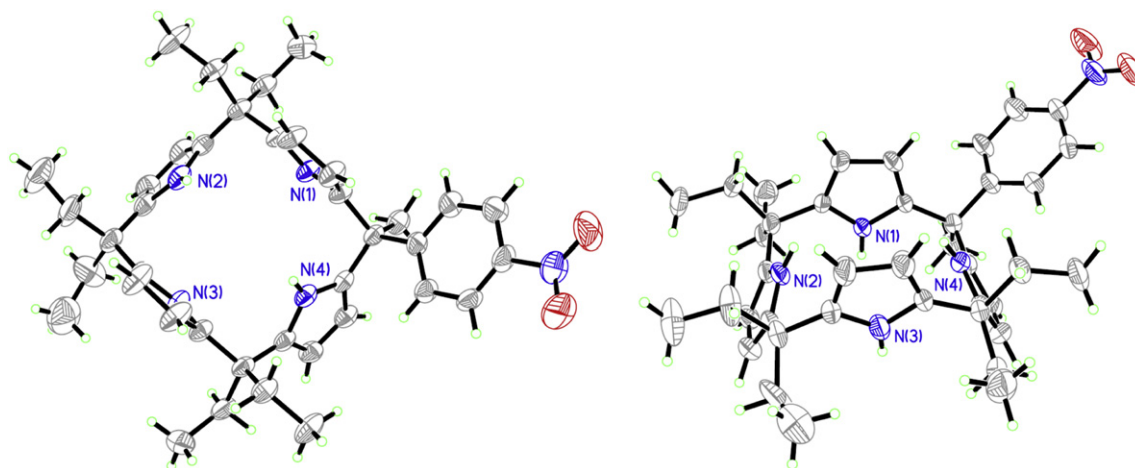


Figure 4. Top view (left) and side view (right) of the X-ray structure of **6** (in CH<sub>3</sub>CN).

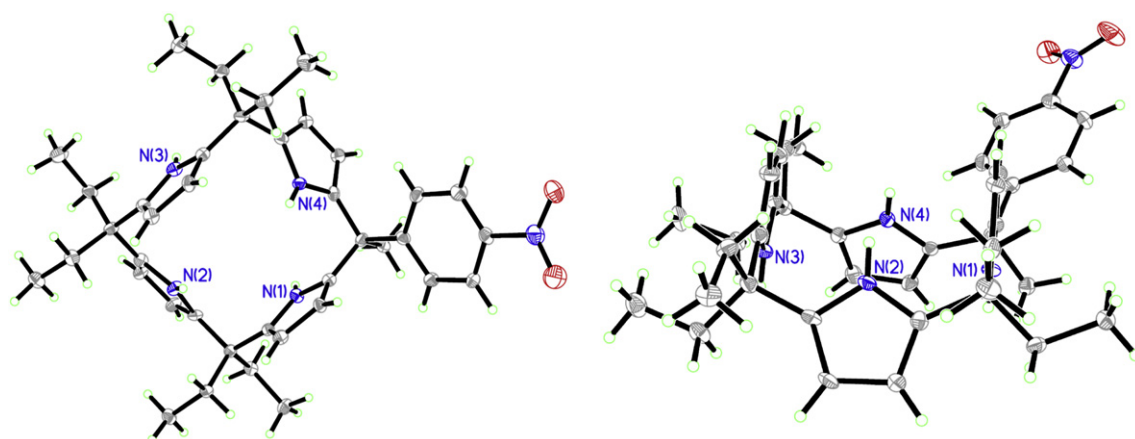
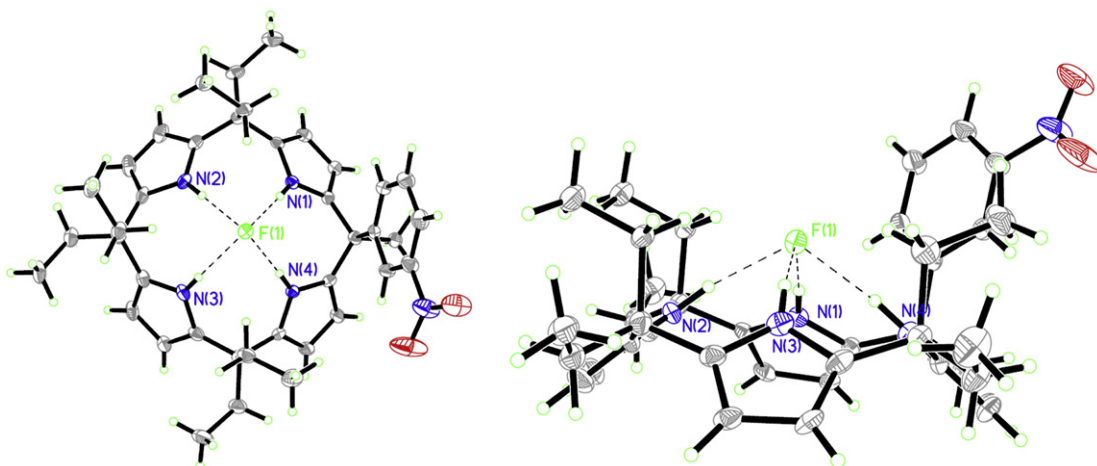


Figure 5. Top view (left) and side view (right) of the X-ray structure of **6** (in acetone).

groups were almost parallel to the calix[4]pyrrole plants, which were like the widespread samples in the four-aromatic *meso*-substituted calix[4]pyrroles<sup>24–26</sup> and the di-aromatic *meso*-substituted calix[4]pyrroles.<sup>25</sup> On the other hand, in some cases of di-aromatic *meso*-substituted calix[4]pyrroles,<sup>26</sup> the aromatic groups were sometimes vertical to the calix[4]pyrrole plant due to the favor in the thermal dynamics.

The single crystals of **5**·F<sup>−</sup> and **6**·F<sup>−</sup> were obtained by the diffusion of *n*-hexane to the CH<sub>2</sub>Cl<sub>2</sub> solutions of **5**-(*n*-Bu)<sub>4</sub>NF and **6**-(*n*-Bu)<sub>4</sub>NF. The two single crystals adopted cone conformations (Figs. 6 and 7), which were the common cases of the almost calix[4]pyrroles–anion complexes<sup>3,4</sup> and some uncomplexed four-aromatic *meso*-substituted calix[4]pyrroles.<sup>8,22,24</sup> There were two kinds of complexes in the crystal of **6**·F<sup>−</sup>, which showed a little



**Figure 6.** Top view (left) and side view (right) of the X-ray structure of **5**·F<sup>−</sup> complex ((*n*-Bu)<sub>4</sub>N<sup>+</sup> counter-ions were omitted for clarity).

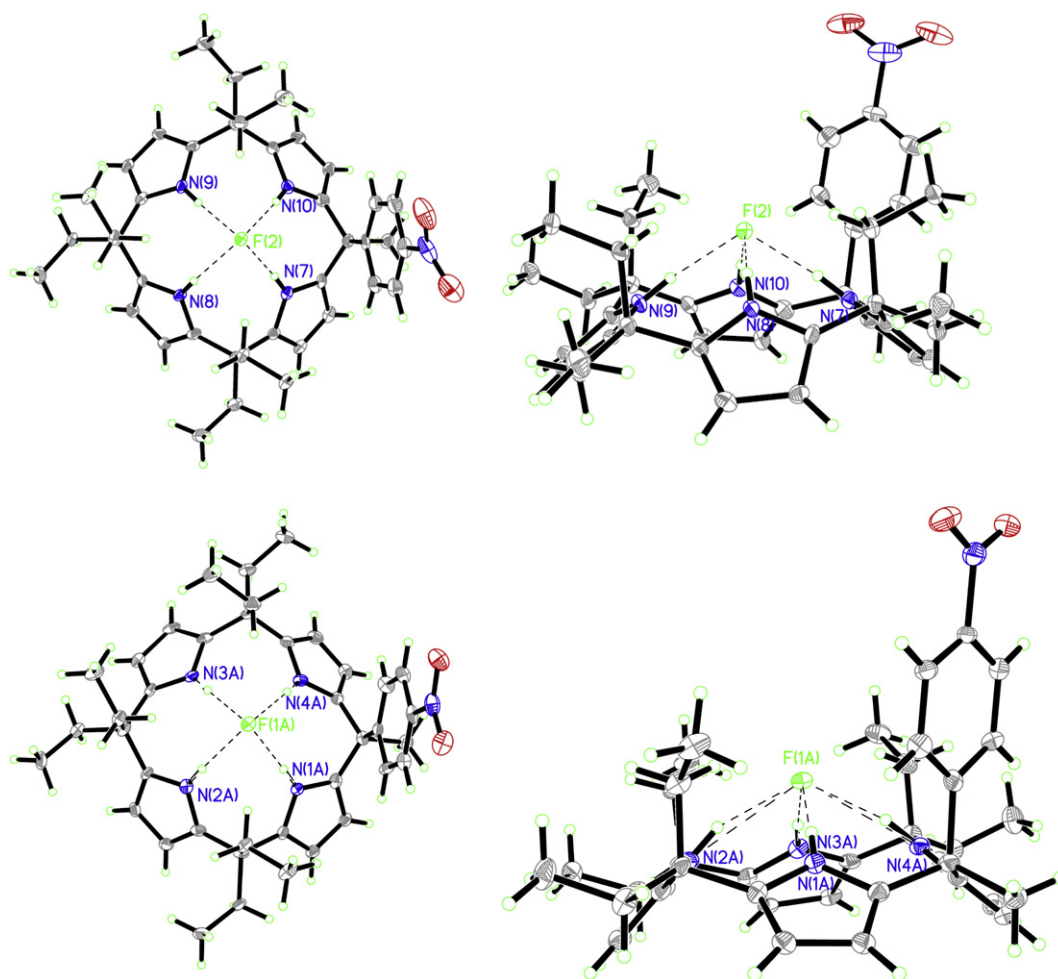


**Figure 7.** Two types of complexes (top view (left) and side view (right)) of the X-ray structure of **6**·F<sup>−</sup> complex ((*n*-Bu)<sub>4</sub>N<sup>+</sup> counter-ions were omitted for clarity).

difference in the orientation of the *meso* ethyl group. However, after investigated in detail, the most attractive features of these crystals were the strange conformations of the phenyl group in the complexes. It is unexpected to find that similar to the free hosts **5/6** the aromatic groups were parallel to the calix[4]pyrrole plant, showing some differences to our former work.<sup>26</sup> Further observation showed that the average pyrrole N–H···F distance of **6** (2.766 Å)

was much shorter than that of **5** (2.788 Å) (Table 2), which illustrated that the binding ability of **6** to the anions was higher than **5**.

## 2.5. Theoretical calculation

In order to explain the strange conformations of the receptors and the complexes, the theoretical investigations were applied by

**Table 2**  
Intermolecular and direct host–guests hydrogen bond parameters for crystals in this study

	D–H...A	<i>d</i> (Å) (H...A)	$\theta$ (°) (D–H...A)	<i>d</i> (Å) (D...A)
<b>5</b> ·F <sup>−</sup>	N1–H1...F1	1.912	170.98	2.785
	N2–H2...F1	1.915	171.12	2.788
	N3–H3...F1	1.987	153.41	2.801
	N4–H4...F1	1.903	173.61	2.779
<b>6</b> ·F <sup>−</sup>	N1–H1...F1	1.874	172.59	2.749 <sup>a</sup>
	N2–H2...F1	1.953	159.60	2.794 <sup>a</sup>
	N3–H3...F1	1.893	172.33	2.767 <sup>a</sup>
	N4–H4...F1	1.887	167.20	2.752 <sup>a</sup>
	N7–H7...F2	1.899	173.30	2.775
	N8–H8...F2	1.984	151.70	2.790
	N9–H9...F2	1.921	172.30	2.796
	N10–H10...F2	1.895	166.25	2.758

<sup>a</sup>  $x-1/2, -y+1/2, z$ .

using semi-empirical method in gas phase. We also constructed the phenyl-horizontal conformation of compounds **5** and **6** and the complexes by rotating the phenyl plant for 90° and −90°. All the single crystals and the constructed conformations were optimization at the B3LYP/3-21G\* level of theory, and the single-point energy was calculated at the B3LYP/6-31G\* level of theory. The stabilization energies were calculated as the difference in the energy between the sum of the receptor and the free fluoride and the complex.

According to our calculated results, the following observations can be made (1) for free hosts, the phenyl-horizontal conformations were the only theoretical optimized results from different initial conformations we constructed, which agree well with our crystal structure. (2) Concerning the complexes, the phenyl-horizontal style was also more favorable than the phenyl-vertical style according to the energy comparison (Fig. 8). For compounds **6**, **5** (nitro-*exo*), and **5** (nitro-*endo*), the phenyl-horizontal style is more stable than phenyl-vertical style by about 1.4, 0.0, and 5.0 kcal/mol in the gas phase, respectively. All these energy changes were small so that the phenyl group may rotate freely. (3) The associate energy of compound **6** (166.3 kcal/mol) was much higher than compound **5** (121.3 kcal/mol), which agrees well with the <sup>1</sup>H NMR titration observations of compound **1/2**. These can be attributed to the large volume of the nitro group, which results in the deviation of the pyrrole N–H and the phenyl group to the anions.

### 3. Conclusion

In summary, two redox anion receptors based on calix[4]pyrrole and ferrocene have been synthesized. The electrochemical investigation revealed that these compounds can respond to the anions with the different shifts of Fc/Fc<sup>+</sup> couple. With the <sup>1</sup>H NMR titration study, the selectivity to F<sup>−</sup> and AcO<sup>−</sup> ions in CD<sub>3</sub>CN solution was confirmed.<sup>27–32</sup> The conformations of the mono-aromatic *meso*-substituted calix[4]pyrroles and their anion complexes in the solid state have been studied, and the rationality of the crystal conformations was proved by theoretical study.

## 4. Experimental

### 4.1. General

<sup>1</sup>H NMR spectra were recorded in CDCl<sub>3</sub>, CD<sub>3</sub>CN, and DMSO, with TMS as an internal standard, on a Varian Mercury Vx300 spectrometer and an Oxford AS400 MHz spectrometer. High resolution mass spectra were recorded on an IonSpec QFT-ESI 7.0 T mass spectrometer. Mass spectra were recorded on a Finnigan LCO

Advantage mass spectrometer. All other commercially available reagents were used without further purification.

## 4.2. Synthesis of receptors

### 4.2.1. Compound 5

3-Nitroacetophenone **7** (1.656 g, 10 mmol), pyrrole (2.7 ml, 40 mmol), and penton-3-one (3.17 ml, 30 mmol) were dissolved in a mixture of methanol and dichloromethane (160 ml, 1:1 v/v), borontrifluoride–etherate (2.58 ml, 20 mmol) was added to the solution, and the mixture was stirred at room temperature for 60 h. The reaction mixture was washed with saturated aqueous NaHCO<sub>3</sub> and brine, and dried over MgSO<sub>4</sub>. The large amount of solvent was moved and the residue was purified by column chromatography over silica gel (eluant: petrol ester/ethyl acetate=30:1) to give **5** (1.104 g, 17.8%) as a yellow powder. <sup>1</sup>H NMR (300 MHz, CDCl<sub>3</sub>)  $\delta$ : 8.06 (1H, d, *J*=7.8 Hz, phenyl C–H), 7.78 (1H, t, phenyl C–H), 7.49–7.46 (1H, m, phenyl C–H), 7.40 (1H, t, phenyl C–H), 7.17 (2H, s, pyrrole N–H), 6.95 (2H, s, pyrrole N–H), 5.95–5.91 (6H, m, pyrrole C–H), 5.63–5.59 (2H, m, pyrrole C–H), 1.91 (3H, s, −CH<sub>3</sub>), 1.87–1.73 (12H, m, −CH<sub>2</sub>−), 0.71–0.59 (18H, m, −CH<sub>3</sub>); <sup>13</sup>C NMR (300 MHz, CDCl<sub>3</sub>)  $\delta$ : 149.8, 148.0, 137.2, 136.1, 135.5, 135.0, 133.5, 128.3, 122.4, 121.6, 106.3, 105.9, 105.1, 104.9, 44.6, 43.0, 29.0, 28.9, 28.5, 28.4, 8.1, 7.9, HRMS (ESI) calcd for C<sub>39</sub>H<sub>50</sub>N<sub>5</sub>O<sub>2</sub>: 620.3959 ([M+H]<sup>+</sup>), found: 620.3962 ([M+H]<sup>+</sup>).

### 4.2.2. Compound 6

4-Nitroacetophenone **7** (1.656 g, 10 mmol), pyrrole (2.7 ml, 40 mmol), and penton-3-one (3.17 ml, 30 mmol) were reacted in accord with the procedure used for the synthesis of **5** and gave **6** (1.035 g, 16.6%) as a yellow powder. <sup>1</sup>H NMR (300 MHz, CDCl<sub>3</sub>)  $\delta$ : 8.07 (2H, d, *J*=9 Hz, phenyl C–H), 7.20–7.17 (4H, m, phenyl C–H and pyrrole N–H), 6.94 (2H, s, pyrrole N–H), 5.94–5.91 (6H, m, pyrrole C–H), 5.64–5.63 (2H, m, pyrrole C–H), 1.89 (3H, s, −CH<sub>3</sub>), 1.86–1.75 (12H, m, −CH<sub>2</sub>−), 0.68–0.61 (18H, m, −CH<sub>3</sub>); <sup>13</sup>C NMR (300 MHz, CDCl<sub>3</sub>)  $\delta$ : 155.0, 146.5, 137.0, 136.1, 135.4, 134.9, 128.3, 122.8, 106.3, 105.8, 105.1, 104.9, 44.9, 43.0, 29.1, 28.9, 28.6, 28.5, 8.1, 8.0; HRMS (ESI) calcd for C<sub>39</sub>H<sub>48</sub>N<sub>5</sub>O<sub>2</sub>: 618.3813 ([M−H]<sup>−</sup>), found: 618.3822 ([M−H]<sup>−</sup>).

### 4.2.3. Compound 3

To the suspension of **5** (0.620 g, 1 mmol) and Pd/C (5%, 0.200 g) in ethanol (40 ml) was added NH<sub>2</sub>NH<sub>2</sub>·H<sub>2</sub>O (80%, 2.0 ml), and the mixture was allowed to heat under reflux for 2 h. Pd/C was removed by the filtration of the reaction mixture while cooling. The filtrate was evaporated to dryness in vacuo. The residue was redissolved in CH<sub>2</sub>Cl<sub>2</sub>, dried over Na<sub>2</sub>SO<sub>4</sub>, and evaporated to dryness. The white solid was purified by column chromatography over silica gel (eluant: dichloromethane/ethyl acetate=50:1) to give **3** (0.469 g, 79.6%) as a white powder. <sup>1</sup>H NMR (400 MHz, CDCl<sub>3</sub>)  $\delta$ : 7.15 (2H, s, pyrrole N–H), 7.04 (1H, t, phenyl C–H), 6.96 (2H, s, pyrrole N–H), 6.68–6.66 (1H, m, phenyl C–H), 6.54 (1H, d, *J*=6.8 Hz, phenyl C–H), 6.45 (1H, s, phenyl C–H), 5.90 (6H, s, pyrrole C–H), 5.67 (2H, s, pyrrole C–H), 1.83 (3H, s, −CH<sub>3</sub>), 1.81–1.74 (12H, m, −CH<sub>2</sub>−), 0.66–0.57 (18H, m, −CH<sub>3</sub>); ESI-MS([M+H]<sup>+</sup>): 590.58.

### 4.2.4. Compound 4

Compound **6** (0.620 g, 1 mmol), Pd/C (5%, 0.200 g), and NH<sub>2</sub>NH<sub>2</sub>·H<sub>2</sub>O (80%, 2.0 ml) were reacted in accord with the procedure used for the synthesis of **3** (eluant: dichloromethane) and gave **4** (0.504 g, 85.5%) as a white powder. <sup>1</sup>H NMR (300 MHz, CDCl<sub>3</sub>)  $\delta$ : 7.17 (2H, s, pyrrole N–H), 7.00 (2H, s, pyrrole N–H), 6.81 (2H, d, *J*=8.4 Hz, phenyl C–H), 6.55 (2H, d, *J*=8.4 Hz, phenyl C–H), 5.91–5.90 (6H, m, pyrrole C–H), 5.67 (2H, s, pyrrole C–H), 3.53 (2H, br s, −NH<sub>2</sub>), 1.87–1.45 (15H, m, −CH<sub>3</sub> and −CH<sub>2</sub>−), 0.66–0.60 (18H, m, −CH<sub>3</sub>); <sup>13</sup>C NMR (300 MHz, CDCl<sub>3</sub>)  $\delta$ : 144.6, 137.8, 137.1, 136.1, 135.9, 135.8, 128.2, 114.4, 105.6, 105.4, 104.9, 43.9, 43.0, 29.2, 29.0, 28.8,

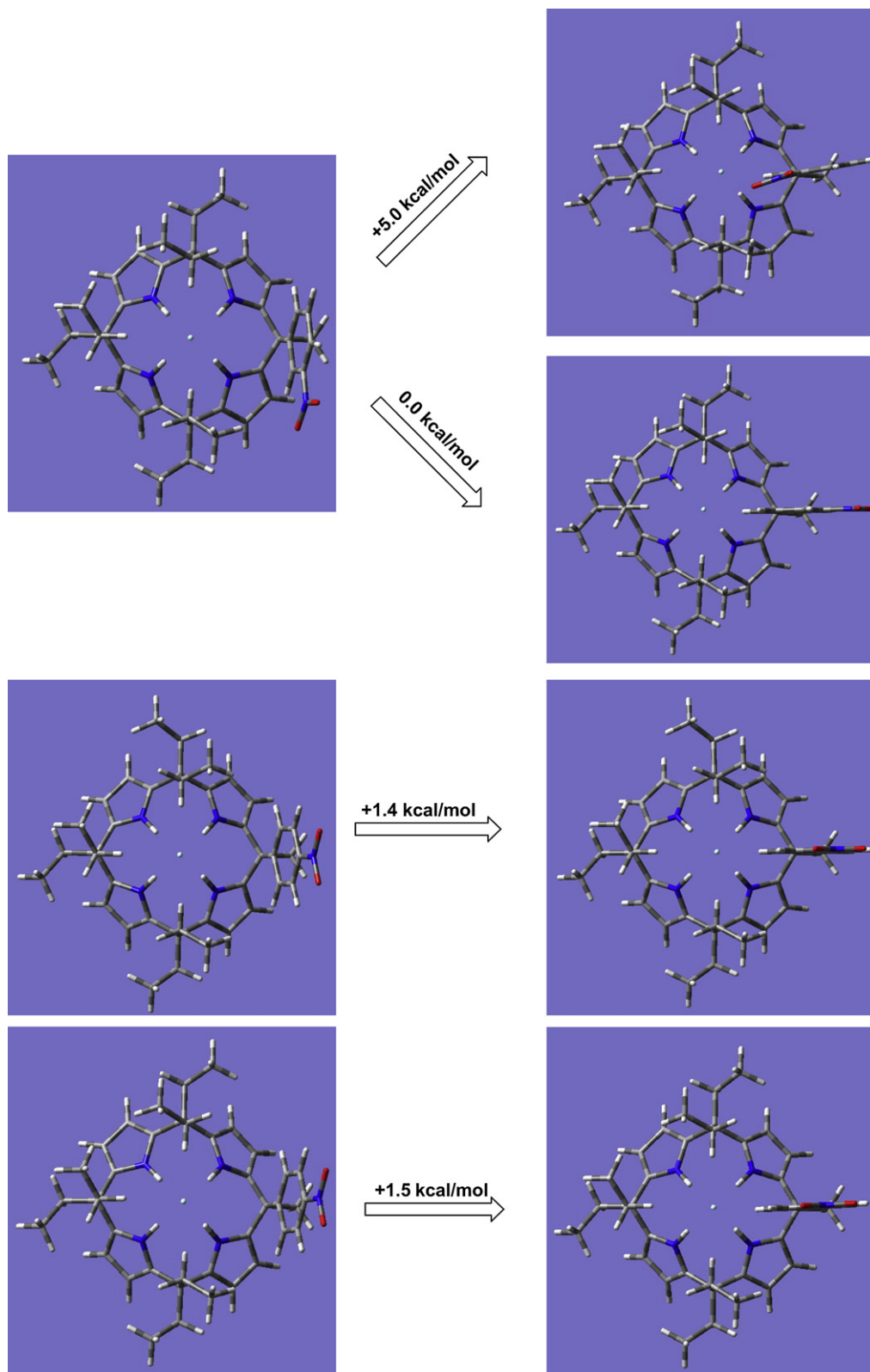


Figure 8. Calculated structure and the energy differences for the 5-F<sup>-</sup> and 6-F<sup>-</sup> models.

28.7, 8.1, 8.0; HRMS (ESI) calcd for C<sub>39</sub>H<sub>50</sub>N<sub>5</sub>: 618.3813 ([M-H]<sup>-</sup>), found: 618.3822 ([M-H]<sup>-</sup>).

#### 4.2.5. Compound 1

A solution of **3** (0.701 g, 1.19 mmol) and pyridine (1.0 ml) in dichloromethane (20 ml) was cooled in an ice-water bath and

ferrocenoyl chloride (0.287 g, 1.16 mmol) was added dropwise. The reaction mixture was stirred for 24 h at room temperature and washed with 40% citric acid, dried over MgSO<sub>4</sub>, and evaporated to dryness in vacuo. The residue was purified by column chromatography over silica gel (eluant: dichloromethane) to give **1** (0.353 g, 38.1%) as an orange solid. <sup>1</sup>H NMR (300 MHz, CD<sub>3</sub>CN) δ: 8.06 (1H, s,

**Table 3**X-ray crystallographic data for **5**, **6** (in CH<sub>3</sub>CN), **6** (in acetone), **5**·F<sup>-</sup>, and **6**·F<sup>-</sup>

	<b>5</b>	<b>6</b> (in CH <sub>3</sub> CN)	<b>6</b> (in acetone)	<b>5</b> ·F <sup>-</sup>	<b>6</b> ·F <sup>-</sup>
CCDC number	675246	675245	675247	675249	675248
Empirical form	C <sub>39</sub> H <sub>49</sub> N <sub>5</sub> O <sub>2</sub>	C <sub>41</sub> H <sub>54</sub> N <sub>6</sub> O <sub>2</sub>	C <sub>45</sub> H <sub>61</sub> N <sub>5</sub> O <sub>4</sub>	C <sub>55</sub> H <sub>88</sub> FN <sub>6</sub> O <sub>3.50</sub>	C <sub>112</sub> H <sub>174</sub> Cl <sub>4</sub> F <sub>2</sub> N <sub>12</sub> O <sub>4</sub>
Formula weight	619.83	662.89	735.99	908.31	1932.43
Crystal system	Monoclinic	Triclinic	Triclinic	Monoclinic	Orthorhombic
Space group	P121/c1	P-1	P-1	P121/n1	Pna21
<i>a</i> (Å)	12.525(3)	10.634(5)	9.5670(15)	12.068(6)	39.100(16)
<i>b</i> (Å)	16.783(3)	13.231(7)	14.600(2)	22.243(11)	11.358(5)
<i>c</i> (Å)	19.490(6)	14.940(8)	16.960(3)	19.911(10)	25.469(11)
α (°)	90	103.196(10)	75.150(18)	90	90
β (°)	123.14(2)	108.839(9)	78.31(2)	97.485(6)	90
γ (°)	90	96.503(10)	72.980(16)	90	90
<i>V</i> (Å <sup>3</sup> )	3430.5(15)	1896.6(16)	2168.6(6)	5300(5)	11311(8)
<i>Z</i>	4	2	2	4	4
<i>D</i> <sub>calcd</sub> (g/cm <sup>3</sup> )	1.200	1.157	1.127	1.138	1.135
μ (mm <sup>-1</sup> )	0.075	0.072	0.072	0.073	0.162
Total reflections	31,606	9858	15,882	39,637	68,050
Unique reflections	8141	6650	7319	9351	19,656
<i>R</i> <sub>1</sub> / <i>wR</i> <sub>2</sub> [ <i>I</i> >2σ( <i>I</i> )]	0.0624/0.1628	0.0626/0.1379	0.1231/0.2468	0.1471/0.2889	0.0898/0.1792
<i>R</i> <sub>1</sub> / <i>wR</i> <sub>2</sub> (all data)	0.0713/0.1707	0.2382/0.2100	0.1778/0.2783	0.1775/0.3055	0.1122/0.1921
GoF on <i>F</i> <sup>2</sup>	1.089	0.921	1.203	1.261	1.132

amide N–H), 7.60 (2H, s, pyrrole N–H), 7.56–7.53 (1H, m, phenyl C–H), 7.35 (2H, br s, pyrrole N–H), 7.30 (1H, t, phenyl C–H), 7.19 (1H, t, phenyl C–H), 6.63 (1H, d, *J*=7.8 Hz, phenyl C–H), 5.88–5.82 (6H, m, pyrrole C–H), 5.75 (2H, t, pyrrole C–H), 4.81 (2H, t, Fc C–H), 4.42 (2H, t, Fc C–H), 4.21 (5H, s, Fc C–H), 1.87–1.81 (15H, m, –CH<sub>3</sub> and –CH<sub>2</sub>–), 0.68–0.55 (18H, m, –CH<sub>3</sub>); <sup>13</sup>C NMR (300 MHz, CD<sub>3</sub>CN) δ: 168.036, 148.895, 138.060, 136.856, 135.968, 135.906, 135.521, 127.548, 122.402, 119.801, 118.464, 104.729, 104.238, 104.177, 70.391, 69.335, 68.143, 44.302, 42.373, 42.312, 27.857, 27.690, 27.530, 26.725, 26.535, 7.199; HRMS (ESI) calcd for C<sub>50</sub>H<sub>58</sub>FeN<sub>5</sub>O: 800.3997 ([M–H]<sup>-</sup>), found: 800.3985 ([M–H]<sup>-</sup>).

#### 4.2.6. Compound 2

Compound **4** (0.834 g, 1.41 mmol), pyridine (1.0 ml), and ferrocenyl chloride (0.301 g, 1.22 mmol) were reacted in accord with the procedure used for the synthesis of **1** (eluant: chloroform/ethyl acetate=20:1) and gave **2** (0.669 g, 59.0%) as an orange solid. <sup>1</sup>H NMR (300 MHz, CD<sub>3</sub>CN) δ: 8.11 (1H, s, amide N–H), 7.61 (2H, m, pyrrole N–H), 7.50 (2H, d, *J*=8.7 Hz, phenyl C–H), 7.32 (2H, br s, phenyl N–H), 6.92 (2H, d, *J*=8.7 Hz, phenyl C–H), 5.87–5.82 (6H, m, pyrrole C–H), 5.71 (2H, t, pyrrole C–H), 4.85 (2H, t, Fc C–H), 4.42 (2H, t, Fc C–H), 4.22 (5H, s, Fc C–H), 1.97–1.83 (15H, m, –CH<sub>3</sub> and –CH<sub>2</sub>–), 0.67–0.56 (18H, m, –CH<sub>3</sub>); <sup>13</sup>C NMR (400 MHz, CD<sub>3</sub>CN) δ: 168.656, 144.097, 137.363, 136.688, 136.377, 136.121, 127.898, 127.770, 119.796, 105.185, 104.752, 104.682, 104.591, 70.928, 69.843, 68.677, 44.433, 42.872, 42.762, 28.427, 28.173, 28.067, 27.074, 26.846, 7.600; HRMS (ESI) calcd for C<sub>50</sub>H<sub>58</sub>FeN<sub>5</sub>O: 800.3997 ([M–H]<sup>-</sup>), found: 800.4007 ([M–H]<sup>-</sup>).

#### 4.3. <sup>1</sup>H NMR titration experimental

The <sup>1</sup>H NMR spectra were recorded on a Varian Mercury Vx300 and Oxford AS400 instrument. In a typical anion titration experiment, aliquots of an anion (tetrabutylammonium fluoride, chloride, bromide, dihydrogenphosphate, acetate, or hydrogen sulfate, 0.25 mol/L CD<sub>3</sub>CN solutions) were added to a 0.5 mL 5 mmol/L solution of receptor; 17 aliquots were added corresponding to 0, 0.1, 0.2, 0.3, 0.4, 0.5, 0.6, 0.7, 0.8, 0.9, 1.0, 1.5, 2.0, 2.5, 3.0, 4.0 and 5.0 equiv of anion. The chemical shift of the pyrrole β-CH on the receptor was monitored as it moved upfield upon addition of anion.

#### 4.4. Electrochemical studies

All electrochemical experiments were carried out using a BAS-100 W electrochemical apparatus in dry acetonitrile solution at

25 °C as described previously. *n*-Bu<sub>4</sub>NPF<sub>6</sub> (0.1 mol/L) was employed as the supporting electrolyte. A standard three-electrode cell consists of a glassy carbon disk as working electrode, a platinum wire as counter electrode, and 0.01 mol/L AgNO<sub>3</sub>/Ag (in 0.1 mol/L *n*-Bu<sub>4</sub>NPF<sub>6</sub>-MeCN) as reference electrode. The ferrocenium/ferrocene redox couple was taken as the internal standard. The reproducibility of the potentials was smaller than 10 mV. All sample solutions were 1×10<sup>-4</sup> mol/L, while the anions (5 equiv) were added to the corresponding receptors.

#### 4.5. DFT calculation

All theoretical calculations were carried out using the Gaussian 03<sup>32</sup> packages mounted on NKStar supercomputer. All the single crystals and the constructed conformations were optimization at the B3LYP/3-21G\* level of theory, and the single-point energy were calculated at the B3LYP/6-31G\* level of theory. The stabilization energies were calculated as the difference in the energy between the sum of the receptor and the free fluoride and the complex.

#### 4.6. X-ray crystallography

The diffraction data were measured on a BRUKER SMART 1000 CCD diffractometer with Mo Kα radiation (λ=0.71073 Å) by ω scan mode. All data were corrected by semi-empirical method using SADABS program. The program SAINT<sup>33</sup> was used for integration of the diffraction profiles. The structure was solved by the direct methods using SHELXS program of the SHELXL-97 package and refined with SHELXL.<sup>34</sup> The final refinement was performed by full matrix least-squares methods with anisotropic thermal parameters for all non-hydrogen atoms of F<sup>2</sup>. The hydrogen atoms of the compounds were placed in the geometrically calculated positions. All hydrogen atoms were included in the final refinement in the riding model approximation with displacement parameters derived from the parent atoms to which they were bonded. Crystallographic data and refinement parameters of the five crystals are summarized in Table 3.

#### Acknowledgements

This project was supported by the Major State Basic Research Development Program of China (Grant no. G2007CB808000). We also thank the computational support of Nankai University ISC and



the technical support of the Center for Theoretical and Computational Chemistry, College of Chemistry of Nankai University.

## References and notes

1. Binachi, A.; Bowman-James, K.; Garcia-Espana, E. *Supramolecular Chemistry of Anion [M]*; Wiley-VCH: New York, NY, 1997.
2. Beer, P. D.; Gale, P. A. *Angew. Chem., Int. Ed.* **2001**, *40*, 486–516.
3. Gale, P. A.; Sessler, J. L.; Král, V. *Chem. Commun.* **1998**, 1–8.
4. Gale, P. A.; Anzenbacher, P., Jr.; Sessler, J. L. *Coord. Chem. Rev.* **2003**, *240*, 191–221.
5. Anzenbacher, P., Jr.; Jursikova, K.; Sessler, J. L. *J. Am. Chem. Soc.* **2000**, *122*, 9350–9351.
6. Song, M.-Y.; Na, H.-K.; Kim, E.-Y.; Lee, S.-J.; Kim, K. I.; Baek, E.-M.; Kim, H.-S.; An, D. K.; Lee, C.-H. *Tetrahedron Lett.* **2004**, *45*, 299–301.
7. Camiolo, S.; Gale, P. A. *Chem. Commun.* **2000**, 1129–1130.
8. Bonomo, L.; Solari, E.; Toraman, G.; Scopelliti, R.; Latronico, M.; Floriani, C. *Chem. Commun.* **1999**, 2413–2414.
9. Turner, B.; Botoshansky, M.; Eichen, Y. *Angew. Chem., Int. Ed.* **1998**, *37*, 2475–2478.
10. Gale, P. A.; Hursthouse, M. B.; Light, M. E.; Sessler, J. L.; Warriner, C. N.; Zimmerman, R. S. *Tetrahedron Lett.* **2001**, *42*, 6759–6762.
11. Turner, B.; Shterenberg, A.; Kapon, M.; Suwinska, K.; Eichen, Y. *Chem. Commun.* **2002**, 404–405.
12. Harmjan, M.; Gill, H. S.; Scott, M. J. *J. Org. Chem.* **2001**, *66*, 5374–5383.
13. Sessler, J. L.; Andrievsky, A.; Gale, P. A.; Lynch, V. *Angew. Chem., Int. Ed.* **1996**, *35*, 2782–2785.
14. Sessler, J. L.; Gebauer, A.; Gale, P. A. *Gazz. Chim. Ital.* **1997**, *127*, 723–726.
15. Sessler, J. L.; Gale, P. A.; Genge, J. W. *Chem.—Eur. J.* **1998**, *4*, 1095–1099.
16. Gale, P. A.; Bleasdale, E. R.; Chen, G. Z. *Supramol. Chem.* **2001**, *13*, 557–563.
17. Wang, Q.; Huang, R. J. *Organomet. Chem.* **2000**, *604*, 287–289.
18. Saki, N.; Akkaya, E. U. *J. Inclusion Phenom. Macrocyclic Chem.* **2005**, *53*, 269–273.
19. Sessler, J. L.; An, D.; Cho, W.-S.; Lynch, V. J. *J. Am. Chem. Soc.* **2003**, *125*, 13646–13647.
20. Hynes, M. J. *J. Chem. Soc., Dalton Trans.* **1993**, 311–312.
21. Gale, P. A.; Sessler, J. L.; Král, V.; Lynch, V. J. *J. Am. Chem. Soc.* **1996**, *118*, 5140–5141.
22. Anzenbacher, P., Jr.; Jursiková, K.; Lynch, V. M.; Gale, P. A.; Sessler, J. L. *J. Am. Chem. Soc.* **1999**, *121*, 11020–11021.
23. Szymańska, I.; Radecka, H.; Radecki, J.; Gale, P. A.; Warriner, C. N. *J. Electroanal. Chem.* **2006**, *591*, 223–228.
24. Woods, C. J.; Camiolo, S.; Light, M. E.; Coles, S. J.; Hursthouse, M. B.; King, M. A.; Gale, P. A.; Essex, J. W. *J. Am. Chem. Soc.* **2002**, *124*, 8644–8652.
25. Bruno, G.; Cafeo, G.; Kohnke, F. H.; Nicolò, F. *Tetrahedron* **2007**, *63*, 10003–10010.
26. Yang, W.; Yin, Z.; Li, Z.; He, J. and Cheng, J.-P. Unpublished.
27. Wang, T.; Bai, Y.; Ma, L.; Yan, X.-P. *Org. Biomol. Chem.* **2008**, *6*, 1751–1755.
28. Wang, Y.-H.; Lin, H.; Lin, H.-K. *Chin. J. Chem.* **2007**, *25*, 1430–1433.
29. Zhang, Y.-M.; Ren, H.-X.; Zhou, Y.-Q.; Luo, R.; Xu, W.-X.; Wei, T.-B. *Turkish J. Chem.* **2007**, *31*, 327–334.
30. Han, F.; Bao, Y.; Yang, Z.; Fyles, M. T.; Zhao, J.; Peng, X.; Fan, J.; Wu, Y.; Sun, S. *Chem. Eur. J.* **2007**, *13*, 2880–2892.
31. Shi, D.-Q.; Wang, H.-Y.; Li, X.-Y.; Yang, F.; Shi, J.-W.; Wang, X.-S. *Chin. J. Chem.* **2007**, *25*, 973–976.
32. Frisch, M. J.; Trucks, G. W.; Schlegel, H. B.; Scuseria, G. E.; Robb, M. A.; Cheeseman, J. R.; Montgomery, J. A., Jr.; Vreven, T.; Kudin, K. N.; Burant, J. C.; Millam, J. M.; Iyengar, S. S.; Tomasi, J.; Barone, V.; Mennucci, B.; Cossi, M.; Scalmani, G.; Rega, N.; Petersson, G. A.; Nakatsuji, H.; Hada, M.; Ehara, M.; Toyota, K.; Fukuda, R.; Hasegawa, J.; Ishida, M.; Nakajima, T.; Honda, Y.; Kitao, O.; Nakai, H.; Klene, M.; Li, X.; Knox, J. E.; Hratchian, H. P.; Cross, J. B.; Bakken, V.; Adamo, C.; Jaramillo, J.; Gomperts, R.; Stratmann, R. E.; Yazyev, O.; Austin, A. J.; Cammi, R.; Pomelli, C.; Ochterski, J. W.; Ayala, P. Y.; Morokuma, K.; Voth, G. A.; Salvador, P.; Dannenberg, J. J.; Zakrzewski, V. G.; Dapprich, S.; Daniels, A. D.; Strain, M. C.; Farkas, O.; Malick, D. K.; Rabuck, A. D.; Raghavachari, K.; Foresman, J. B.; Ortiz, J. V.; Cui, Q.; Baboul, A. G.; Clifford, S.; Cioslowski, J.; Stefanov, B. B.; Liu, G.; Liashenko, A.; Piskorz, P.; Komaromi, I.; Martin, R. L.; Fox, D. J.; Keith, T.; Al-Laham, M. A.; Peng, C. Y.; Nanayakkara, A.; Challacombe, M.; Gill, P. M. W.; Johnson, B.; Chen, W.; Wong, M. W.; Gonzalez, C.; Pople, J. A. *Gaussian 03, Revision C.01*; Gaussian: Wallingford, CT, 2004.
33. Bruker AXS. *SAINT Software Reference Manual*; Bruker: Madison, WI, 1998.
34. Sheldrick, G. M. *SHELXTL NT, Program for Solution and Refinement of Crystal Structures, version 5.1*; University of Göttingen: Göttingen, Germany, 1997.